Diagnostic measurements of CUEBIT based on the dielectronic resonance process

E. Takacs, T. D. Kimmel, K. H. Brandenburg, R. K. Wilson, A. C. Gall, J. E. Harriss, and C. E. Sosolik

Citation: AIP Conference Proceedings **1640**, 154 (2015); doi: 10.1063/1.4905414
View online: http://dx.doi.org/10.1063/1.4905414
View Table of Contents: http://scitation.aip.org/content/aip/proceeding/aipcp/1640?ver=pdfcov
Published by the AIP Publishing

Diagnostic Measurements of CUEBIT Based on the Dielectronic Resonance Process

E. Takacs[1, a)], T. D. Kimmel[1], K. H. Brandenburg[1], R. K. Wilson[1], A. C. Gall[1], J. E. Harriss[1], C. E. Sosolik[1]

[1]*Department of Physics and Astronomy Clemson University Clemson, SC 29634*

[a)] Corresponding author: etakacs@clemson.edu

Abstract. In this paper we report the first observation of x-ray radiation from the new Clemson University Electron Beam Ion Trap (CUEBIT). The analysis of the emitted dielectronic recombination x-ray photons from highly charged argon ions allowed us to probe parameters specific to the ion cloud inside the machine. Argon dielectronic resonances could provide a standard method to cross-compare the electron beam and ion cloud characteristics of different devices.

INTRODUCTION

Dielectronic excitation is a resonant atomic process where an electron in the continuum gets captured to a bound orbital of an ion with the simultaneous promotion of an initially bound electron to an excited state. This doubly excited state is the quantum state of a one lower charge state ion. The system can then decay via autoionization, which is the inverse process of dielectronic excitation, or by the emission of a photon leaving the ion in the lower charge state. The latter route is therefore called dielectronic recombination (DR) and it is an important atomic process affecting the ionization balance in hot plasmas [e.g. 1-9].

Devices that operate by the use of a well-defined energy electron beam are ideally suited for the study of dielectronic resonance excitation processes. Electron cooler facilities, for example in ion storage rings, have been successfully used to map low-energy resonances [2-4]. Electron beam ion trap (EBIT) and electron beam ion source (EBIS) type devices, with their high-energy electron beams, have been proven to be effective at investigating higher energy DR processes [5-12]. In particular, EBITs are usually equipped with observation ports perpendicular to the electron beam axis, therefore the appearance of DR photons provide a clear signature of the process [5-9].

The new CUEBIT facility at Clemson University is equipped with an x-ray observation port perpendicular to the direction of the electron beam. In a series of x-ray experiments that present the first observation x-rays from the CUEBT, we have studied dielectronic resonance transitions in highly charged argon ions in order to study the properties of the CUEBIT highly charged ion plasma.

In this paper we present our results in the systematic variation of the neutral gas pressure in the source region and show the changing ion trapping conditions inside the machine. We point out that the dielectronic resonance process is an effective method in understanding the properties of the ion cloud and is ideally suited for the systematic diagnosis of EBIT(S) type devices. We suggest that the observation of argon dielectronic resonances could provide a standard method to cross-compare the electron beam characteristics of different devices.

Proceedings of the XII International Symposium on Electron Beam Ion Sources and Traps
AIP Conf. Proc. 1640, 154-160 (2015); doi: 10.1063/1.4905414

CLEMSON UNIVERSITY ELECTRON BEAM ION TRAP (CUEBIT) AND EXPERIMENTAL SETUP

The new electron beam ion trap facility at Clemson University consists of an EBIS-SC (DREEBIT GmbH) type ion source and a beamline equipped with beam transport and charge state selection elements. The ion source is horizontally oriented to easily connect to the horizontal beamline and extraction system. Properties of the beamline and first measurements with extracted highly charged ions are presented elsewhere [13]. In this paper we focus on the ion source and present the first in-trap spectroscopy results.

The ion source accommodates a heated electron gun that can provide electron currents up to 250-300 mA. The electron gun structure can be floated to a maximum potential of -6 kV. Coupled with a maximum of 20 kV drift tube voltage, the device should be capable of accelerating electrons to energies up to 26 keV. These nominal energies are sufficient to produce most of the ion charge states across the periodic table.

The drift tube section of the device has an intermediate length between typical EBIT and EBIS type devices, with a trap region of about 20 cm in length. Sections of the drift tube can be biased separately to allow for the adjustment of trap depth and the operation of the machine in static or pulsed mode.

Surrounding the drift tubes are a pair of superconducting magnets in a Helmholtz-type arrangement capable of producing a 6T magnetic field along the axis of the machine. The magnets are kept at liquid helium temperature utilizing a closed cycle cryocooler system, which reduces the cost of operation of the machine.

The source is equipped with potentially two spectroscopic observation ports on opposite sides of the machine. Currently, only one of these ports is utilized and is equipped with a 125 micrometer thin beryllium window. This configuration allows for the transmission of x-rays generated by the highly charged ion plasma created and trapped by the electron beam.

The CUEBIT is equipped with a gas injection system that consists of a computer controlled precision needle valve and a perforated tube along the length of the middle drift tube to allow neutral atoms to enter the trap region for ionization.

In our present experiment, neutral argon atoms were injected into the source, and preselected levels of overall source pressures were maintained throughout the systematic measurements. The electron beam energy was adjusted between the values of approximately 2.0 keV to 3.2 keV, which covers the region of the K dielectronic resonances in argon ion charge states with initial L shell vacancies.

For the observation of the emitted x-rays we utilized a 10 mm^2/4 mm (area/thickness) Princeton Gamma-Tech IGX cryogenic solid-state germanium detector optimized and calibrated for low energy x-ray detection. The detector was installed on the observation port, and allowed for the detection of x-rays emitted at 90 degrees with respect to the electron beam direction. The instrument has a thin polymer window that allows the full transmission of x-rays that escape the beryllium window of the EBIT to be observed. Our spectral region of interest was at the Kα emission region of Ar near the 3 keV x-ray energy [10-12, 14-16]. We have selected an energy window wide enough to allow the Kα lines of the different argon charge states to be detected and analyzed. Our measurements were relative in a sense that we compared emitted intensities relative to one another, therefore geometrical and anisotropic emission effects cancel out in our analysis.

DIAGNOSTICS USING KLL DIELECTRONIC RESONANCES IN HE-LIKE AR

The energy resolution of the CUEBIT electron beam is high enough (approximately 30-60 eV depending on the trap conditions) to allow for the separation of the KLL dielectronic resonances produced from different charge states of argon as it is shown on Figure 1. In this diagnostic work we wanted to focus on a single charge state component of the plasma, and selected the $1s2s2p$ and $1s2p^2$ He-like Ar resonances for this purpose. In this section we discuss the diagnostic value of the He-like resonance structure, and point out how different physical properties of the ion cloud are related to the observable properties of the resonance peaks.

Calculations and high-resolution experiments showed that the He-like Ar resonance structure could be fitted with three Gaussian peaks corresponding to the $1s2s2p$ and $1s2p^2$ KLL resonances [16].

In our analysis, the free fitting parameters were the space charge shift of the energy position of the resonances, the overall x-ray intensity of the resonances, the common width of the DR peaks, and a constant background corresponding to the competing radiative recombination (RR) process in the region.

The constraints applied were the separation of the three resonances (fixed by values obtained from the NIST atomic spectra database [17]), that the resonance width be the same for all three peaks, and that the space charge shift of the different peaks were energy dependent according to Eqn 1 [12].

$$\Delta(E_e) = \Delta(E_0)\sqrt{\frac{E_e}{E_0}} \tag{1}$$

In Equation 1, $\Delta(E_0)$ is the space charge shift of the lowest energy $1s2s2p$ resonance at $E_0 = 2169$ eV and $\Delta(E_e)$ is the space charge shift of a resonance at E_e. Common relative intensity ratios of the resonant peaks were applied to all fits.

X-ray Emission Intensity – Peak Height

The overall emitted x-ray intensity is representative of the number of trapped He-like argon ions in the trap. In order to determine absolute ion numbers the knowledge of geometrical factors are needed. These depend on the properties of the electron beam and ion cloud, and the geometry of the detector arrangement. For absolute numbers, the electron beam as well as the extent and density of the ion cloud can be modeled or measured experimentally. The measured x-ray intensity also needs to be corrected for the non-isotropic emission of the process [18].

In relative measurements, the peak heights generated under different EBIT conditions can be compared, and the geometrical factors can be neglected to a first order approximation. Higher order corrections require detailed models, but at the same time provide further diagnostic value.

In summary we can claim that *the relative change in the overall emitted DR x-ray intensity can be interpreted as the change in the number of He-like ions in the trap* as has been previously discussed in e.g. [19].

Electron Energy Width of the Resonance – Peak Width

The natural line widths of all of the resonances concerned are very small; on the order of a tenth of an eV [14-16]. As a result, the measured DR widths correspond to the broadening of the sharp resonances due to the broadened energy distribution of the electron beam in the interaction region.

The energy of the electron beam inside the EBIT is determined by the potential difference between the cathode of the electron gun (where the electrons are generated) and the middle drift tube (where the electrons interact with the ions). Voltage jitters in the power supply can be minimized and only have a small effect in comparison with the space charge potential of the combined electron beam and ion cloud inside the machine.

The calculation of the space charge potential of the electron beam is straightforward if the shape of the beam can be modeled or measured experimentally. This potential is the major component in the axial trapping of the ions inside the EBIT. The contribution of the space charge of the ion cloud is not as trivial however, as the extent of the ion cloud delicately depends on the different heating and cooling processes taking place inside the machine. Heating is mainly caused by Coulomb collisions with energetic electrons and the cooling is provided by the evaporation of the different interacting ion species within the trap [20].

With the ion cloud temperature modeled or estimated, the size and shape of the ion cloud, along with the resulting radial potential that includes both the electrons and the ions in the trap, can be calculated in a self-consistent manner. The ion cloud, due to its elevated temperature, is always larger than the size of the electron beam. As a result, full neutralization of the charges inside the trap can never be achieved. Neutralization factors of 70-80% are generally assumed [20].

Considering the above, *in general, a changing DR width at a fixed electron beam current is an indication for a changing ion cloud temperature inside the trap*. Larger widths indicate higher ion cloud temperatures as ions also interact with electrons at the outer edge of the beam.

Position of the Resonance – Peak Centroid

The energy of a dielectronic resonance is determined by the discrete energy level structure of a particular ion. The positions of the KLL dielectronic resonances in He-like Ar for example can be calculated from the tabulated He-like and Li-like energy levels of Ar that are documented in the NIST Atomic Spectral Database [17]. These resonance energy positions have also been used in previous experiments [11-12, 14-16].

As discussed in the previous section the total energy of the electron beam is mainly determined by the voltage difference between the electron gun and ion trap. However, it is also affected by the space charge potential, which is the sum of the electron current dependent beam potential and the ion cloud potential. The space charge potential not only broadens the resonance width, but also results in an overall shift of the position of the DR position.

In general, the position of the DR peak in terms of the applied drift tube voltage can be associated with the electron beam neutralization factor: the ratio of the number of ions to the number of electrons in the trap.

EXPERIMENTAL RESULTS

With a new EBIT on hand at Clemson University, we are putting effort into the understanding of the machine's operating conditions. Our modeling efforts, considering the effects outlined above, are under way and we have started a series of systematic measurements to experimentally determine plasma cloud conditions inside the CUEBIT. Our first set of measurements included in this paper regard the systematic change of the gas pressure inside the source.

The gas injection system provided by the device maker company DREEBIT consists of a computer controlled precision needle valve and a perforated tube along the length of the middle drift tube, injecting neutral gases towards the center of the machine. The recommended operation of the gas injection system is based on a feedback loop that controls the overall pressure in the source region through a pressure gauge connected to this section of the machine.

With an overall base background pressure of 4×10^{-10} mbar, we have systematically changed the feedback controlled source pressure. Our measurements ranged between 6×10^{-9} mbar (the recommended operating pressure of the CUEBIT for low charge state production), down to as close as we could get to the base background pressure with the feedback loop still operational at 7×10^{-10} mbar.

We have covered an electron energy range (without space charge correction) from about 2.2 keV to 2.6 keV in order to observe KLL dielectronic resonances in argon ions with L shell vacancies. Figure 1 shows the varying x-ray intensity as the beam energy is scanned over the KLL dielectronic resonance region at 2.5×10^{-9} mbar gas injection pressure. We have selected an x-ray energy range near 3 keV that included the Kα transitions in all of these charge states. The observed resonance structure is due to the different charge state argon ions in the trap.

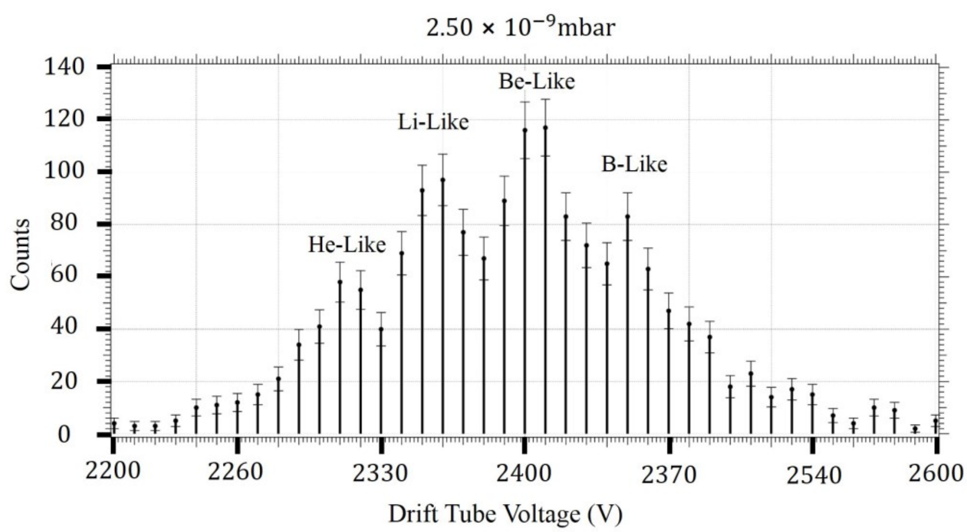

FIGURE 1. The resonance peaks of different charge states in the ion cloud at 2.50×10^{-9} mbar source pressure.

As described above in our analysis, we have focused our efforts on the KLL dielectronic resonances in He-like Ar. Based on the tabulated positions of the resonance peaks and previous high-resolution measurements, we have included three Gaussian peaks in our fits, as previously explained. One of these is a dominant resonance ($1s2p^2$), and the other two give smaller contributions on the lower energy wing of the major peak. Our overall fits gave reasonable χ-square values and satisfactory agreement with experimental data with the constraints mentioned in the previous section. The free fitting parameters were a constant background, the space charge shift of the main resonance peak, and the common width of the resonances. Figures 2 (a) and (b) show the fits of the He-like Ar DR resonances at different source pressures.

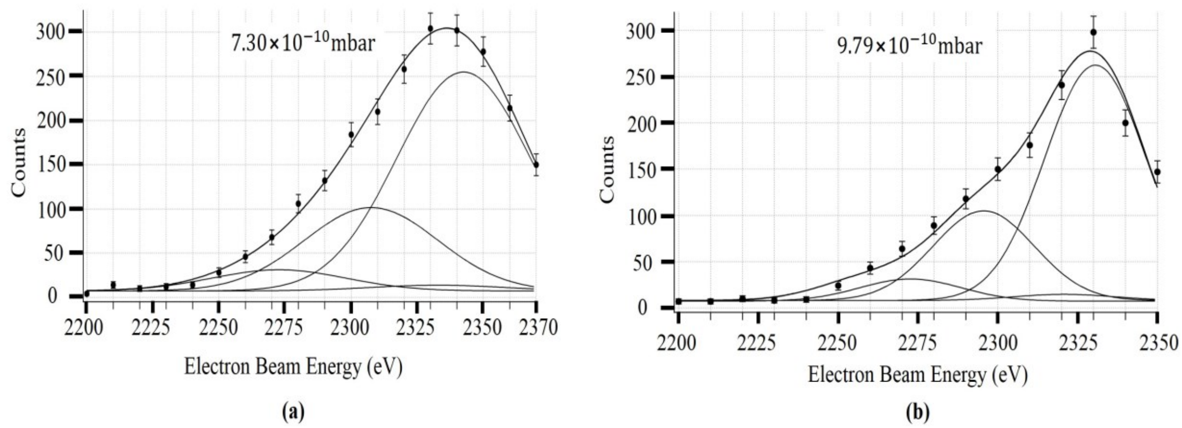

FIGURE 2. He-like Ar resonance structure at two different source pressures. (a) 7.3×10^{-10} mbar and (b) 9.79×10^{-10} mbar.

DISCUSSION

The results, as a function of the CUEBIT source pressure, are included in Figures 3 (a-c). In Figure 3 (a) we see a systematic change of the space charge potential correction as a function of the gas injection pressure. Figure 3 (b) indicates a decreasing trend in the width of the ion cloud suggesting the presence of colder ions at higher pressures. Figure 3 (c) shows the continuous decrease of the number of He-like resonance x-ray photons with the increasing gas pressure.

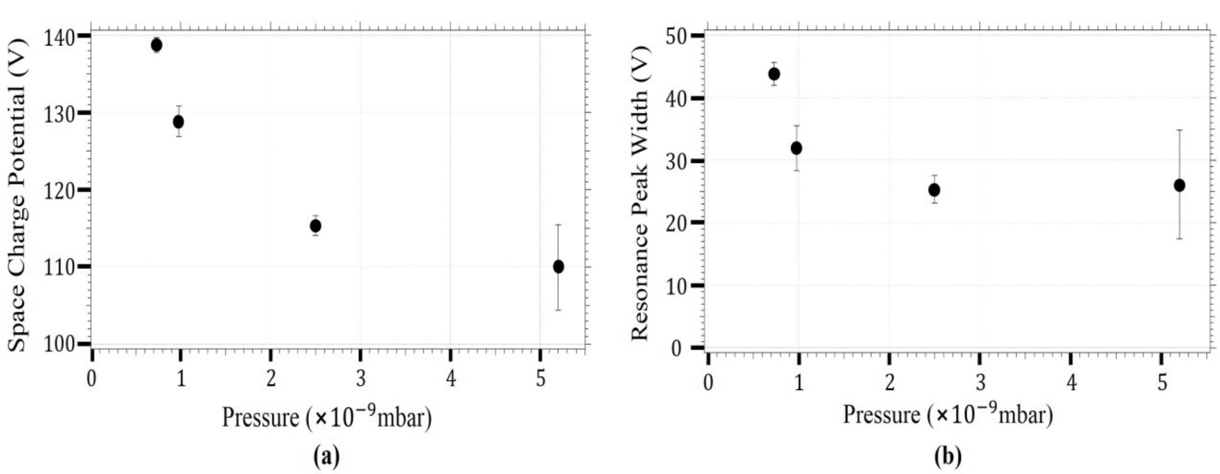

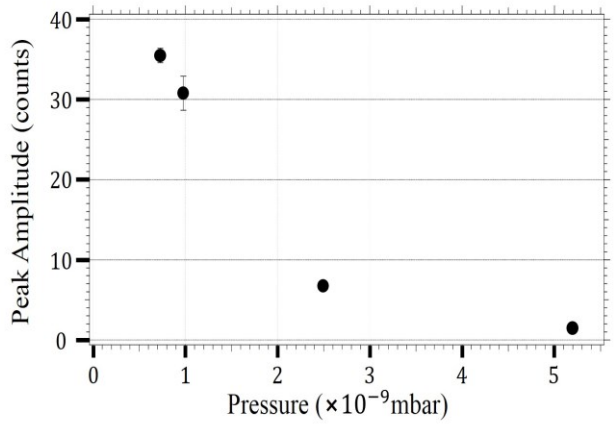

(c)

FIGURE 3. Pressure dependent DR peak parameters. (a) space charge shift, (b) resonance width, (c) DR peak amplitude.

The trend in the space charge potential shift indicates a change in the electron beam neutralization by the ion cloud. With a fixed electron beam current of about 100 mA, the change of the composition of the ion cloud, as a result of recombination with neutral atoms, provides different amounts of cooling to the cloud. This results in a changing overall ion cloud temperature, indicated by the shift of the resonance position on Figure 3 (a). Detailed modeling of the ongoing processes are under way, but already this trend shows the need of lower gas injection pressures, when the goal is the generation of higher charged ion clouds.

The changing resonance width in Figure 3 (b) is in agreement with the arguments for different ion cloud temperatures. The resonance widths also indicate colder ion temperatures at higher pressures. The width seems to be very sensitive to the ion cloud temperatures, therefore it will be an independent way of checking our models. Once confirmed, this could be a useful tool in diagnosing the temperature of the plasma in EBITs.

The correlation between gas pressure and number of x-ray photons is expected. An increase in pressure results in an increase of the number of neutral particles injected into the EBIT. In the regime where charge exchange is the dominant process determining the charge state balance, this will result in a decreased number of higher charge state ions. By removing the geometrical factors as previously discussed, the intensity can be used to diagnose the relative number of ions in the trap.

CONCLUSIONS

The measurements taken for the purposes of this paper were not time intensive (about one hour per dataset). By evaluating the fitting parameters outlined above, this experimental procedure may be used to diagnose the number of ions and the ion cloud temperature in the trap, as well as the electron beam neutralization factor. Once additional modeling and experiments have been completed, our current fitting parameters can be verified and refined.

ACKNOWLEDGMENTS

This work was supported in part by the Clemson University Creative Inquiry (CI) Program.

Taylor D. Kimmel, Kristyn H. Brandenburg, R. Kevin Wilson were supported by the University Professional Internship & Co-Op (UPIC) program. It is one of the student engagement initiatives associated with Clemson University's 2020 Road Map.

Taylor D. Kimmel and Kristyn H. Brandenburg would like to thank the Clemson University Department of Physics and Astronomy for the opportunity and funding to attend the EBIST 2014 conference.

The authors acknowledge the support of the National Science Foundation (NSF-DMR-0960100).

REFERENCES

1. T. Kallman, AIP Conference Proceedings **1545** (2013) 164
2. S.Ali, S. Mahmood, I. Orban, Z.Altun, and Reinhold Schuch, Phys. Scr. **T156** (2013) 014049
3. S. Schippers, Journal of Physics: Conference Series **388** (2012) 012010
4. A. Mueller, Eur. Phys. J. Special Topics **169** (2009) 35
5. Yu. Ralchenko, J.D. Gillaspy, J. Reader, D. Osin, J.J. Curry and Y.A. Podpaly, Phys. Scr. **T156** (2013) 014082
6. P. Beiersdorfer, M.J. May, J.H. Scofield, S.B. Hansen, High Energy Density Physics **8** (2012) 271
7. D.J. McLaughlin, Y. Hahn, E. Takacs, E.S. Meyer, and J.D. Gillaspy, Phys. Rev. A **54** (1996) 2040
8. J. Xiao, C. Han, K. Yao, Y. Shen, Y. Yang, B. Wei, Y. Fu, D. Lu, R. Hutton, and Y. Zou, AIP Conference Proceedings **1545** (2013) 73
9. H. Watanabe, A.P. Kavanagh, H. Kuramoto, Y.M. Li, N. Nakamura, S. Ohtani, B.E. O'Rourke, A. Sato, H. Tawara, X.M. Tong, F.J. Currell, Nuclear Instruments and Methods in Physics Research B **235** (2005) 261
10. J. P. Briand and P. Charles, J. Arianer, H. Laurent, C. Goldstein, J. Dubau, M. Loulergue, and F. Bely-Dubau, Phys. Rev. Lett. **52** (1984) 617
11. R. Ali, C. P. Bhalla, C. L. Cocke, and M. Stockli, Phys. Rev. Lett. **64** (1990) 633
12. R. Ali, C.P. Bhalla, C.L. Cocke, M. Schulz, and M. Stockli, Phys. Rev. A **44** (1991) 223
13. R. Shyam, D.D. Kulkarni, D.A. Field, E.S. Srinadhu, D.B. Cutshall, W.R. Harrell, J.E. Harriss and C.E. Sosolik, Present Proceedings
14. Y. Zou, J.R. Crespo Lopez-Urrutia, and J. Ullrich, Phys. Rev. A **67** (2003) 042703
15. D.R. DeWitt, D. Schneider, M.W. Clark, M.H. Chen, and D. Church, Phys. Rev. A **44** (1991) 7185
16. A. J. Smith, P. Beiersdorfer, K. Widmann, M. H. Chen, and J. H. Scofield, Phys. Rev. A **62** (2000) 052717
17. A. Kramida, Yu. Ralchenko, J. Reader, and NIST ASD Team (2013). NIST Atomic Spectra Database (version 5.1), [Online]. Available: http://physics.nist.gov/asd [Friday, 18-Jul-2014 15:41:14 EDT]. National Institute of Standards and Technology, Gaithersburg, MD
18. C.P. Bhalla, K.R. Karim, M. Wilson, Nuclear Instruments and Methods in Physics Research B **56/57** (1991) 324
19. W. Zhang, K. Yao, Y. Yang, C. Chen, R. Hutton, and Y. Zou, Phys. Rev. A **82** (2010) 020702(R)
20. E. Takacs, J.D. Gillaspy, in: F. Anderegg et al. (Eds.), Non-Neutral Plasma Physics IV, AIP Conf. Proc. Ser. 606, 2002.